Energetic Neutral Atoms from the Heliosheath

P. Wurz*, A. Galli*, S. Barabash† and A. Grigoriev†

*Physics Institute, University of Bern, CH-3012 Bern, Switzerland
†Institute for Space Physics, IRF, S-98128 Kiruna, Sweden

Abstract.
We present the measurement and analysis of hydrogen energetic neutral atoms (ENAs) recorded with the ASPERA-3 instrument on board Mars Express during the cruise phase and the Mars orbit phase. We conclude that the origin of these ENAs is the inner heliosheath. The ENA energy spectra are all very similar and can be fitted well by a two-component power law. The ENA fluxes, integrated from 0.3 keV to 10 keV, vary in the range of $5 \cdot 10^3$ to 10^5 cm^{-2} sr^{-1} s^{-1}. The present ENA data fit together well with earlier ENA data at higher energies, which have their origin also in the inner heliosheath. Comparison of the measured ENA energy spectra with results from several heliospheric models show that some of these models predict significantly lower ENA fluxes at Earth orbit.

INTRODUCTION

The Sun is the source of a supersonic flow of plasma, the solar wind, that fills all interplanetary space, and which rams into the local interstellar medium (LISM) resulting in a large interaction region. The interaction region comprises the solar wind termination shock, where the solar wind is slowed down to subsonic speeds, the heliopause separating solar wind plasma from interstellar plasma, and the bow shock (if it exists). Because of the relative motion of the solar system with respect to the LISM with 26 km/s interstellar neutral atoms can pass the heliopause and penetrate into the solar system, even down to Earth orbit. The termination shock has been identified by the Voyager 1 instrumentation to be at 94 AU during late 2004 [1, 2, 3].

Heliospheric energetic neutral atoms (ENAs) are predominantly hydrogen atoms that have been produced on the far side of the termination shock in the inner heliosheath, the area between the termination shock and the heliopause. There, ENAs are continually produced by charge exchange between interstellar neutral atoms and protons from the solar wind, from pickup ions, or from other ion populations [e.g. 4, 5]. These processes are thought to result in a flux of inward moving ENAs detectable at Earth orbit originating from the inner heliosheath [5, 6, 7]. Imaging these ENAs and measuring their energy spectra provides information on the termination shock, the heliosheath surrounding it, and in general about the interaction of the heliosphere with the local interstellar medium. The IBEX mission of NASA will be recording spatially and spectrally resolved ENA images with a large instrument sensitivity [8].

ENA imaging has become an established means of remote sensing of plasma distributions in planetary and space science [9] and even the lowest ENA energies are now accessible with suitable detection techniques [10]. In the following we will present ENA

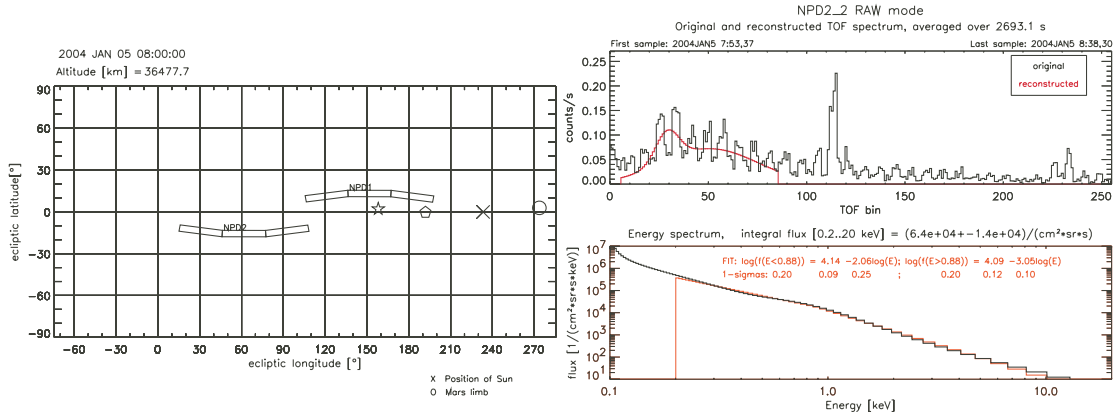

FIGURE 1. Left: Typical observation geometry for the measurement of interstellar ENAs in Mars orbit with MEX being at 36'478 km altitude. The six boxes show the fields of view of the NPD channels, the circle shows the Mars limb, the "X" the position of the Sun, the pentagon the position of the Earth, and the asterisk shows the position of Jupiter. Right: Recorded TOF spectrum (top panel) of the NPD2 channel pointing at 30° longitude and −12° latitude, and the derived energy spectrum together with a fit (bottom panel).

data recorded with the ASPERA-3 instrument on the Mars Express mission of the European Space Agency (ESA).

NPD/ASPERA-3 OBSERVATIONS

The ASPERA-3 instrument on the Mars Express spacecraft has been designed to study the interaction of the solar wind with the Martian atmosphere and to characterize the plasma and neutral particle environment in the vicinity of Mars [11]. The ASPERA-3 instrument comprises four different sensors. The Ion Mass Analyzer and the Electron Spectrometer to measure local ion and electron densities, respectively, and the Neutral Particle Detector (NPD) and the Neutral Particle Imager (NPI) to detect energetic neutral atoms. The results presented here are restricted to neutral particle measurements.

The Neutral Particle Detector consists of two identical sensors NPD1 and NPD2 that are sensitive to ENAs in the energy range from 0.1 to 10 keV using the time-of-flight technique. Each NPD sensor has one start and three stop surfaces that provide an angular resolution of roughly 30° in azimuthal direction and 4° in elevation direction, the latter defined by the entrance system. Together, these six azimuth channels give an instantaneous field of view of NPD of 180°× 4° (see left panel of Fig. 1 for illustration). The energy and the mass of an incident particle can be reconstructed from the time of flight between start and stop surface and from the pulse height of the stop signal. Principally, this design enables us to distinguish oxygen from hydrogen ENAs.

Interstellar ENAs were observed with the NPD sensor of the ASPERA-3 instrument in the energy range from 200 eV to 10 keV during the cruise phase and also in orbit around Mars. The entire data set of NPD data was searched and 51 energy spectra were identified that were attributed to energetic hydrogen atoms originating in the inner

heliosheath [12]. The typical flow direction of these particles is toward the Sun (see left panel of Fig. 1). In short there are the following findings:

- All energy spectra of interstellar ENAs are very similar in shape and are best described by a two-component power-law. The average parameters for the spectra are a first slope $f \propto E^{-1.61}$, a second slope of $f \propto E^{-3.31}$, and the roll-over at $E = 0.77$ keV. See bottom right panel of Fig. 1 for an example.
- The total ENA fluxes integrated over energy of these spectra are highly variable, with measured values from $F_{\mathrm{ENA}} = 5 \cdot 10^3$ cm^{-2} s^{-1} sr^{-1} to $F_{\mathrm{ENA}} = 1.5 \cdot 10^5$ cm^{-2} s^{-1} sr^{-1}, with the former being the detection threshold. The mean ENA flux is $F_{\mathrm{ENA}} = 3.5 \cdot 10^4$ cm^{-2} s^{-1} sr^{-1}.
- Heliospheric ENA fluxes are observed for all ecliptic longitudes. The integrated ENA fluxes show an enhancement by a factor of two in the anti-apex (tailward) direction of the LISM flow.
- Data from the interplanetary cruise to Mars, during which most of these measurements were performed, show less scatter than data recorded in Mars orbit, the latter probably resulting from contaminations by ENAs of martian origin.
- A preliminary analysis of NPD/ASPERA-4 cruise phase data from the Venus Express mission is in full agreement with the NPD/ASPERA-3 data from the Mars Express mission. A dedicated observation program is planned for the Venus Express mission once nominal operations are resumed.

We conclude that these ENAs originate from the heliosheath. We checked carefully to exclude the following alternative or background sources as a possible source for the observed signal:

- There is no correlation of the ENA signal with nearby UV bright stars coming into the field of view of the NPD sensor. Moreover, the background spectra caused by UV photons are completely different from spectra of a particle signal.
- There is no correlation with planets (Earth, Mars, Jupiter) since measurements where a planet was in or near the field-of-view of the instrument were not considered in the analysis (see left panel of Fig. 1 for pointing).
- Neutralized ions of co-rotating interaction regions (CIR) can be ruled out as a source for these ENAs because the ion fluxes needed in the CIRs to account for the observed ENAs fluxes is three orders of magnitude higher than actual CIR fluxes.
- A solar wind related origin has been investigated, e.g. correlation with Parker angle, and can be ruled out. Note that the flow direction of these ENAs is towards the Sun.

In addition, the maximum of this ENA flux found in the anti-apex direction of the interstellar gas argues against a local origin of these ENAs. This is because within a distance of few AU of the Sun the interstellar hydrogen density is higher in the apex than in the anti-apex direction due to the photoionization by solar UV light. Note that there is no hydrogen focussing cone in the anti-apex direction. The helium focussing cone cannot cause this maximum either, because the charge exchange cross section between hydrogen and helium at energies of 1 keV is very small [7].

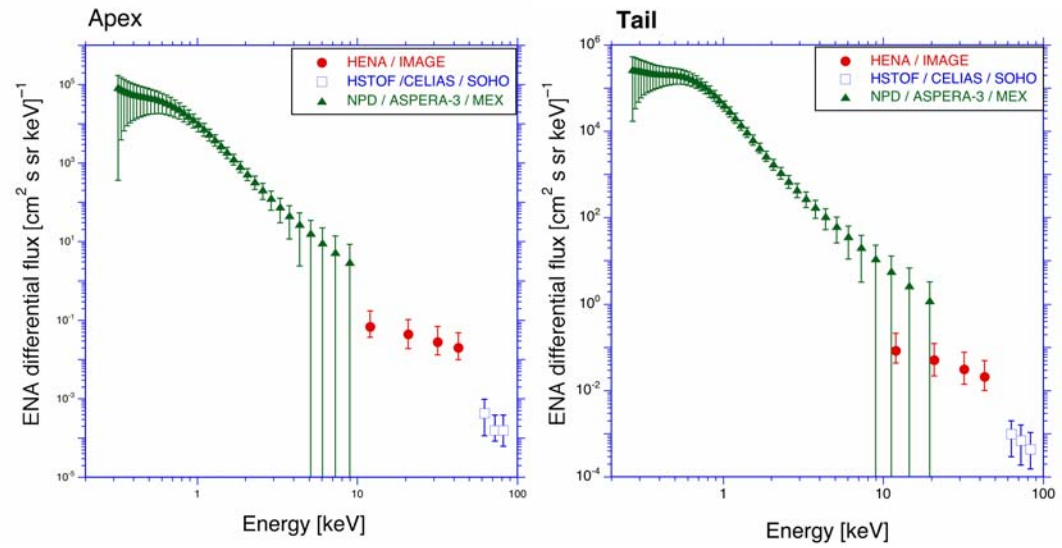

FIGURE 2. Compilations of ENA measurements for various energies. Data points are from the NPD sensor of ASPERA-3 on Mars Express [12], from the HENA instrument on IMAGE [13, 14], and from the HSTOF sensor of the CELIAS instrument on SOHO [15]. The HENA data are upper limits. Lines indicate different NPD measurements.

Hydrogen atoms arriving at Mars orbit from the heliosheath have travel times ranging from 0.3 a to 2.4 a for the energy range covered by the NPD measurements. Thus, most of the temporal variations in the ENA flux at the TS will smear out by the time they arrive at Mars and the similarity of the observed energy spectra is not surprising. The variations in ENA flux on the time scale of months we observe are explained by loss of incoming ENAs because of charge exchange with solar wind protons. Given the $1/r^2$ fall-off of the solar wind density this charge exchange is very localized, e.g. within a few AU of Mars. The time scale of these ENA flux variations is commensurate with this range for typical solar wind speeds, although the sampling of the ENA measurements is not good enough to make a definitive statement.

ENAS FROM THE INNER HELIOSHEATH

As discussed above, we interpret the ENA measurements reported above as energetic hydrogen atoms arriving from region of the inner heliosheath. In addition to the NPD measurements there are two more data sets available, one from the HENA instrument on IMAGE [13, 14] and one from the HSTOF sensor of the CELIAS instrument on SOHO [15]. These measurements are shown in Fig. 2 for the apex and the tail direction, left and right panel, respectively. The NPD data points are from the cruise phase from day 10 July 2003 and 14 October 2003, for the apex and tail direction, respectively. Note that the total ENA flux measured with NPD is on average about a factor of two higher in the tailward direction [12]. The reported HENA data are only upper limits [13] and for the HSTOF data sets for several ecliptic longitudes exist [15]. For the latter data set also an

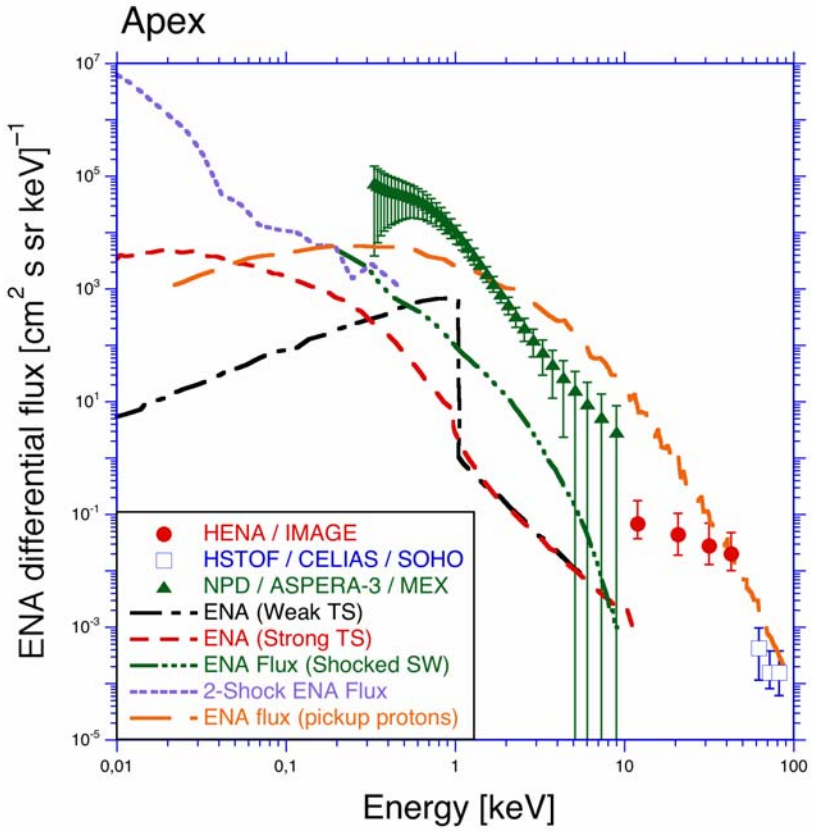

FIGURE 3. Calculated ENA-H energy spectra together with the measurements from Fig. 2. The dashed line and the dashed-dotted line are from [8] for a strong and a weak TS, respectively, the dotted line is data from a two-shock model [17], the dash-dot-dot-dot line shows data from [5], and the long-dashed curve show data from [4].

enhancement by a factor of two in the tailward direction has been reported.

Most of what we know from the region beyond the termination shock is the result of detailed model calculations. These calculations not only predict the shape and the physical parameters in the four regimes of the heliospheric interface, but they also predict energy spectra of ENAs produced in that region and travelling inward to Earth orbit. Several calculated ENA energy spectra for an observer at Earth orbit are reproduced in Fig. 3 [4, 5, 8, 17], together with the ENA measurements reported in Fig. 2. There is a large range in the ENA flux predictions by the various models as can be seen in Fig. 3. Moreover, most of these model calculations, with one exception, considerably underestimate the ENA flux arriving from the heliosheath when compared to the present measurements. Note that most of the NPD measurements are concerned with ENA emission from the martian environment, where the measured ENA fluxes and theoretical predictions agree fairly well. The comparison of the shape of the measured ENA energy spectrum with model calculations from [8] suggests a strong shock, however using the same model calculations the ENA enhancement we find in the tail suggests a weak shock. The Voyager-1 energetic particle data also suggest a weak termination shock [3]. Probably the physical processes of ion acceleration in the heliosheath are more complicated than

is covered by present models.

CONCLUSIONS

In this paper we reported the first detection of ENAs that most plausibly originate in the inner heliosheath. The energy spectra of these heliospheric ENAs are all very similar, and are well described by a two-component power-law with a mean roll-over at 770 eV. Extrapolating these energy spectra to higher energies results in a good agreement with IMAGE/HENA and CELIAS/HSTOF data. Comparison of our ENA measurements with theoretical models show that the fluxes predicted by these models typically are between one and two orders of magnitude lower than the measured ENA fluxes.

The reported heliospheric ENA fluxes have to be compared with optical measurements of hydrogen densities from the heliosphere [18]. The Lyman-α line profile measurements of nearby stars show absorptions features at the red wing of the line caused by heliospheric hydrogen, which are in the velocity range of up to 100 km/s corresponding to energies of about 50 eV of the hydrogen atoms. Since our ENA measurements end at energies of 300 eV we cannot directly compare with the optical measurements. However, if one would extend the measured ENA energy spectrum flatly down to 10 eV there would be additional absorption in the Lyman-α line profile, which is not observed. Thus, one has to assume a drop-off of the ENA spectrum at lower energies. The IBEX mission will have the capability to measure ENAs in this energy range and will answer this question.

ACKNOWLEDGMENTS

The information on the heliospheric Ly-α absorption by B. Wood is gratefully acknowledged. The ASPERA-3 experiment on the European Space Agency (ESA) Mars Express mission is a joint effort between 15 laboratories in 10 countries, all sponsored by their national agencies. We thank all these agencies as well as the various departments/ institutes hosting these efforts. This work is supported by the Swiss National Science Foundation.

REFERENCES

1. L.F. Burlaga, N.F. Ness, M.H. Acuña, R.P. Lepping, J.E.P. Connerney, E.C. Stone, and F.B. McDonald, "Crossing the Termination Shock into the Heliosheath: Magnetic Fields", *Science*, **309**, 2027–2029, (2005).
2. R.B. Decker, S.M. Krimigis, E.C. Roelof, M.E. Hill, T.P. Armstrong, G. Gloeckler, D.C. Hamilton, and L.J. Lanzerotti, "Voyager 1 in the Foreshock, Termination Shock, and Heliosheath", *Science*, **309**, 2020–2024, (2005).
3. E.C. Stone, A.C. Cummings, F.B. McDonald, B.C. Heikkila, N. Lal, and W.R. Webber, "Voyager 1 Explores the Termination Shock Region and the Heliosheath Beyond", *Science*, **309**, 2017–2020, (2005).

4. S.V. Chalov, H.J. Fahr, and V.V. Izmodenov, "Evolution of pickup proton spectra in the inner heliosheath and their diagnostics by energetic neutral atom fluxes", *J. Geophys. Res.*, **108(A6)**, 1266, doi:10.1029/2002JA009492 (2003).
5. H.-J. Fahr and K. Scherer, "Energetic neutral atom fluxes from the heliosheath varying with the activity phase of the solar cycle", *ASTRA Astrophys. Space Sciences Trans.*, **1**, 3–15 (2004).
6. H.S. Hsieh, K.L. Shih, J.R. Jokipii, and M.A. Gruntman, "Sensing the solar-wind termination shock from Earth's orbit", Proceedings of *Solar Wind Seven*, 3rd COSPAR Colloquium, Goslar, Germany, 365–368, (1992).
7. M. Gruntman, E.C. Roelof, D.G. Mitchell, H.J. Fahr, H.O. Funsten, and D.J. McComas, "Energetic neutral atom imaging of the heliospheric boundary region", *Jou. Geophys. Res.*, **106**, 15767–15782, (2001).
8. D. McComas, F. Allegrini, P. Bochsler, M. Bzowski, M. Collier, H. Fahr, H. Fichtner, P. Frisch, H. Funsten, S. Fuselier, G. Gloeckler, M. Gruntman, V. Izmodenov, P. Knappenberger, M. Lee, S. Livi, D. Mitchell, E. Moebius, T. Moore, D. Reisenfeld, E. Roelof, N. Schwadron, M. Wieser, M. Witte, P. Wurz, and G. Zank, "The Interstellar Boundary Explorer (IBEX)," *AIP Conference Proceedings*, **719**, 162–181 (2004).
9. P. Wurz, "Detection of Energetic Neutral Particles," in *The Outer Heliosphere: Beyond the Planets*, edited by K. Scherer, H. Fichtner, and E. Marsch, Copernicus Gesellschaft e.V., Katlenburg-Lindau, Germany, (2000), pp. 251–288.
10. P. Wurz, J. Scheer, and M. Wieser, "Particle scattering off surfaces: application in space science," *e-Jou. Surf. Science Nanotechn.*, **4**, 394–400 (2006).
11. S. Barabash, R. Lundin, H. Andersson, J. Gimholt, M. Holström, O. Norberg, M. Yamauchi, K. Asamura, A.J. Coates, D.R. Linder, D.O. Kataria, C.C. Curtis, K.C. Hsieh, B.R. Sandel, A. Fedorov, A. Grigoriev, E. Budnik, M. Grande, M. Carter, D.H. Reading, H. Koskinen, E. Kallio, P. Riihela, T. Säles, J. Kozyra, N. Krupp, S. Livi, J. Woch, J. Luhmann, S. McKenna-Lawlor, S. Orsini, R. Cerrulli-Irelli, A. Mura, A. Milillo, E. Roelof, D. Williams, J.-A. Sauvaud, J.-J. Thocaven, D. Winningham, R. Frahm, J. Scherer, J. Sharber, P. Wurz, and P. Bochsler, "The Analyzer of Space Plasmas and Energetic Atoms (ASPERA-3) for the Mars Express Mission," *ESA-SP*, **1240**, 121–139 (2004).
12. A. Galli, P. Wurz, S. Barabash, A. Grigoriev, R. Lundin, Y. Futaana, H. Gunell, M. Holmström, E.C. Roelof, C.C. Curtis, K.C. Hsieh, A. Fedorov, J.D. Winningham, R.A. Frahm, R. Cerulli-Irelli, P. Bochsler, N. Krupp, J. Woch, and M. Fraenz, "Direct Measurement of Energetic Neutral Hydrogen in the Interplanetary Medium," *Astrophys. Jou.*, in press (2006).
13. E. Roelof, private comm. (2005).
14. R. Kallenbach, M. Hilchenbach, S.V. Chalov, J.A. Le Roux, and K. Bamert, "On the "injection problem" at the solar wind termination shock", *Astron. Astrophys.*, **439**, 1–22, (2005).
15. M. Hilchenbach, K.C. Hsieh, D. Hovestadt, B. Klecker, H. Grünwaldt, P. Bochsler, F.M. Ipavich, F. Gliem, W.I. Axford, H. Balsiger, W. Bornemann, A. Bürgi, M.A. Coplan, A.B. Galvin, J. Geiss, G. Gloeckler, S. Hefti, D.L. Judge, R. Kallenbach, P. Laeverenz, M.A. Lee, S. Livi, G.G. Managadze, E. Marsch, E. Möbius, M. Neugebauer, H.S. Ogawa, K.U. Reiche, M. Scholer, M.I. Verigin, B. Wilken, and P. Wurz, "Detection of 55–80 keV Hydrogen Atoms of Heliospheric Origin by CELIAS/HSTOF on SOHO," *Astrophys. Jou.*, **503**, 916–921 (1998).
16. E. Möbius, M. Bzowski, H.-R. Müller, and P. Wurz, "Effects in the Inner Heliosphere Caused by Changing Conditions in the Galactic Environment," in *The Solar System, Heliosphere, and the Galactic Environment of the Sun*, edited by P. Frisch, Springer, (2006), in press.
17. G. Zank, private comm. (2003).
18. B.E. Wood, S. Redfield, J.L. Linsky, H.-R. Müller, and G. Zank, "Stellar Lyα emission lines in the Hubble Space Telescope archive: Intrinsic line fluxes and absorption from the heliosphere and astrospheres," *Astrophys. Jou. Suppl. Ser.*, **159**, 118–140, 2005.